Section A-Research paper

NUMERICAL RESULTS OF BINGHAM NON-NEWTONIAN FLUID FLOW IN THE ENTRANCE PART OF CONCENTRIC ANNULI ALONG WITH OUTER WALL ROTATION

Gayathri devi Nangineni[1], N. Sinivasa Rao[2*] and M. Venkata Subba Rao[3]

[1] Research Scholar, Department of Mathematics, School of Applied Science and Humanities, Vignan's Foundation for Science, Technology and Research, Vadlamudi, Andhra Pradesh - 522 213, India
[1]Email: ngayathridevi55@gmail.com

[2]Division of Mathematics, Department of Basic Science and Humanities, GMR Institute of Technology, Rajam, Vizianagaram, A.P, India - 532127
[2]Email: srinivasarao.n@gmrit.edu.in

[2]Department of Mathematics, School of Applied Science and Humanities, Vignan's Foundation for Science, Technology and Research, Vadlamudi, Andhra Pradesh - 522 213, India
[3]Email: mail2mvsr@gmail.com

Abstract:

Numerical research has been done on entrance region flow of Bingham non-Newtonian fluid in a concentric with an annulus revolving exterior walls. Internal cylinder is thought to be motionless when rotating outer cylinder at a fixed angular velocity ω, the pressure P distribution in the radial direction R and the velocity components $U, V,$ and W are obtained using finite difference analysis. The momentum, continuity equations are solved repeatedly by the finite difference method under the boundary layer assumptions of Prandtl. For a variety of non-Newtonian flow qualities and geometrical elements, computational results are achieved. Analysis has been done on the evolution of the pressure distribution, profile of tangential velocity, profile of radial velocity, and profile of axial velocity in the entrance area. The results of the current study were compared with those reported in the literature for different specific cases, similarly they were determined to be consistent.

Keywords: Bingham fluid, Entrance region, concentric annulus, Finite difference method.

1. Introduction

When developing cooling mechanisms for electric machines, uses in engineering for tiny spinning heat exchangers, Practical significance can be seen in the issue of entrance area

flow in circular annuli of rotating exterior walls. Industries involved in polymer manufacturing, axial-flow turbo machinery, and combustion chambers. When operating at low power, a coolant flow rates decrease, laminar flow conditions develop in the field of nuclear reactors. Many significant industrial fluids are referred to be rheological fluids because they have non-Newtonian flow properties. These include paints, glues, inks, meals, polymer solutions, blood, different suspensions like coal-water or coal-oil slurries, and so many others. A fluid under consideration the Bingham model is seen here, it's in the same category of fluids with "time-independent yield stress."

Numerous writers have researched the issue of entry area level flow of non-Newtonian fluids in annular cylinders. "Mishra et al. [1] investigated the flow of the Bingham plastic fluids in the concentric annulus and obtained results for the thickness of the boundary Layer, the center core velocity, and the pressure distribution". "[2] The stress – strain relation for the Casson fluid in the annular space between two coaxial rotating cylinders where the inner cylinder is at rest and outer cylinder is rotating is developed by Batra and Bigyani Das". "Maia and Gasparetto [3] studied a finite difference method for the Power law fluid in the annuli and found differences in the entrance geometries. Sayed-Ahmed and Hazem [4] investigated a finite difference method to study the laminar flow of Power-Law fluid in the concentric annuli with rotating inner wall". For the Herschel-Bulkley Fluids, Kandaswamy and Srinivas Rao [5] have looked into entrance region flow in circular annulus with a rotating inner cylinder.

Furthermore, "Kandasamy [6] shows the entrance region flow heat transfer in concentric annuli for a Bingham fluid and presents the velocity distributions, temperature and pressure in the entrance region". [7] Through concentric annulus, Round with Yu examined the evolving Herschel-Bulkley fluid flows. Batra with Jena [8] investigated assuming blood to follow casson fluid. "Recently, Rekha and Kandasamy [9] studied the entrance region flow of Bingham fluid in an annular cylinder". Schlichting and Gersten K[10] analyzed Boundary layer theory. "Coney and El-shaarawi[11] analyzed A contribution to the computational solution of developing laminar flow in the entrance area of concentric annuli with rotating inner walls". "[12] Flow of casson fluid between two rotating cylinders is developed by R.L.Batra and Bigyanidas".

The issue of Bingham fluid entry region flow in concentric annuli has been researched in the current work. Inner cylinder is assumed to be at rest, and outer cylinder is assumed to be rotating during the analysis. Boundary layer assumptions of Prandtl allow for the discretization and solution of the equation of conservation of mass and momentum using the linearized implicit finite difference method. The resulting system of linear algebraic equations has been solved using the Gauss-Jordan method. For various values of non-Newtonian fluid flow properties as well as geometrical measurements, its development of axial, radial, tangential velocity profiles and the distribution of pressure in the entrance area

level has been calculated. These have an impact on the pressure distribution and velocity profiles, which are discussed.

NOMENCLATURE

l	Consistency index($p_{a.s}$),
m	Radial growth in the numerical mesh network
p	Pressure (p_a),
p_0	Primary pressure (p_a)
P	Dimensionless pressure, $(p-p_0)/(\rho u_0^2)$,
ϵ	Radial coordinate (m),
η	Axial coordinate (m),
θ	Tangential coordinate (rad),
$R=\epsilon/R_1$	Dimensionless radial coordinate,
$Z=2z(1-N)/R_1R_e$	A dimensionless axial coordinate,
R_1, R_2	An inner, outer cylinder's radius (m),
$B=\tau_0R_1/(kl)$	Bingham number,
R_e= $2\rho(R_2-R_1)u_0/l$	Reynolds value,
T_a	Taylor number,
$S=R_1/R_2$	The annular dimensionless ratio,
v_z	Components of velocity in the z direction (m/s),
v_r	Components of velocity in the r direction (m/s),
v_θ	Components of velocity in the θ direction (m/s),
u_0	(m/s) uniform inlet velocity
$U=v_z/u_0$	In the z direction, is a dimensionless velocity component.
$V=\rho v_r R_2/\mu_r$	In the r direction, is a dimensionless velocity component.
$W=v_\theta/v_\theta R_1$	In the θ direction, is a dimensionless velocity component.
ρ	Density of the fluid (kg/m^3),
μ	Apparent viscosity of the model ($p_{a.s}$),
τ_0	Yield stress (p_a),
ω	(rad/s) Regular angular velocity,
$\Delta R, \Delta Z$	Mesh size is dimensionless in the radial, axial direction.

2. Problem Formulation

Figure 1 depicts the problem's geometry. With inner and outer radii, Bingham's non-Newtonian fluid enters the R_1, R_2 horizontal concentric annuli, respectively, by a sizable space with a starting pressure p_0 and a uniform flat velocity profile u_0 along the axial direction z. While the outer cylinder turns at the angular velocity ω, the inner cylinder is resting. The flow is laminar, incompressible, axisymmetric and of constant physical properties.

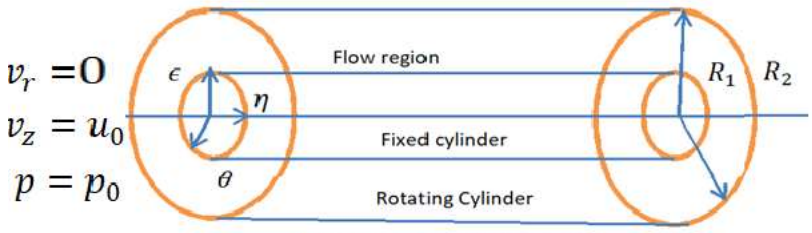

Figure 1.Geometry of the problem

We take into account a cylindrical polar coordinate system with the origin at the inlet section on the annulus's central axis, the z-axis running along it, and the radial direction ϵ running perpendicular to it. With the aforementioned hypotheses and the typical prandtl's boundary layer hypotheses [12] Schlichting and Gersten analyzed Boundary layer theory. A polar coordinate system's governing equations (ϵ, θ, η) for a non-Newtonian Bingham fluid are listed below in the entrance region.

The equation of constitutive for the Bingham fluid is given by Bird et al. [13]

$$\tau_{ij} = \left(\mu + \frac{\tau_0}{\varepsilon}\right)\varepsilon_{ij} \qquad (\tau > \tau_0) \tag{1}$$

Where $\tau = \sqrt{\frac{1}{2}\tau_{ij}\tau_{ij}}$ *and* $\varepsilon = \sqrt{\frac{1}{2}\,\varepsilon_{ij}\varepsilon_{ij}}$

Where τ_{ij} is the stress tensor and ε_{ij} is the rate of strain tensor τ_0 is the yield stress and fluid velocity is μ.

The equation of continuity: $\frac{\partial(\epsilon v_r)}{\partial \epsilon} + \frac{\partial(\epsilon v_z)}{\partial \eta} = 0$ (2)

r-momentum equation: $\frac{\omega^2}{\epsilon} = \frac{1}{\rho}\frac{\partial p}{\partial \epsilon}$ (3)

θ-momentum equation : $v_r\frac{\partial v_\theta}{\partial \epsilon} + v_z\frac{\partial v_\theta}{\partial \eta} + \frac{v_r v_\theta}{\epsilon} = \frac{1}{\rho\epsilon^2}\frac{\partial}{\partial \epsilon}(\epsilon^2\left[\tau_0 + l\epsilon\,\frac{\partial}{\partial \epsilon}\left(\frac{v_\theta}{\epsilon}\right)\right])$ (4)

z-momentum equation : $v_r\frac{\partial v_z}{\partial \epsilon} + v_z\frac{\partial v_z}{\partial \eta} = -\frac{1}{\rho}\frac{\partial p}{\partial \eta} + \frac{1}{\rho}\frac{\partial}{\partial \epsilon}(\epsilon[\tau_0 + l\frac{\partial v_z}{\partial \epsilon}])$ (5)

where ρ is the fluid density, l is the consistency index pressure is p. The velocity components v_z, v_r, v_θ are measured in the directions η, ϵ, θ respectively.

The problem's initial conditions are provided by

For $\eta \geq 0$ and $\epsilon = R_1$, $v_r = v_z = v_\theta = 0$

For $\eta \geq 0$ and $\epsilon = R_2$, $v_r = v_z = 0$ and $v_\theta = \omega R_2$

For $\eta = 0$ and $R_1 < \epsilon < R_2$,$v_z = u_0$ at $\eta = 0, p = p_0$ (6)

The equation of continuity (2) can be stated in the next integral form using the boundary conditions (6):

$$2\int_{R_1}^{R_2} \epsilon v_z \, d\epsilon = (R_2^2 - R_1^2)u_0 \tag{7}$$

The preceding dimensionless variables and the parameters should really be mentioned.

$$R = \frac{\epsilon}{R_2}, \quad U = \frac{v_z}{u_0}, \quad V = \frac{\rho v_r R_2}{\mu_r}, W = \frac{v_\theta}{\omega R_2}, \; S = \frac{R_1}{R_2}, \; P = \frac{p-p_0}{\mu_r}, \quad Z = \frac{2z(1-S)}{R_2 Re},$$

$$B = \frac{\tau_0 R_2}{l u_0}, Re = \frac{2\rho(R_2-R_1)u_0}{l}, \; \mu_r = l\left(\frac{\omega R_1}{R_2}\right), \; T_a = \frac{2\omega^2\rho^2 R_1^2 (R_2-R_1)^3}{\mu_r^2(R_1+R_2)}$$

B is for the Bingham number in this context, Re for Reynolds number, T_a for Taylor number, μ_r for reference viscosity, and S for annulus' aspect ratio.

The dimensionless forms of equations (2) through (5) and (7) are provided by

$$\frac{\partial V}{\partial R} + \frac{V}{R} + \frac{\partial U}{\partial Z} = 0 \tag{8}$$

$$\frac{W^2}{R} = \frac{1}{2}\frac{(1-S)Re^2}{T_a(1+S)}\frac{\partial P}{\partial R} \tag{9}$$

$$V\frac{\partial W}{\partial R} + U\frac{\partial W}{\partial Z} + \frac{VW}{R} = \frac{\partial^2 W}{\partial R^2} + \frac{1}{R}\frac{\partial W}{\partial R} - \frac{W}{R^2} + \frac{2B}{R} \tag{10}$$

$$V\frac{\partial U}{\partial R} + U\frac{\partial U}{\partial Z} = -\frac{\partial P}{\partial Z} + \frac{1}{R}\frac{\partial U}{\partial R} + \frac{\partial^2 U}{\partial R^2} + \frac{B}{R} \tag{11}$$

$$2\int_S^1 RU \, dR = (1 - S^2) \tag{12}$$

The dimensionless form's boundary conditions (6) are as follows:

As $Z \geq 0$, $R = N$, $V = U = W = 0$

As $Z \geq 0$, $R = 1$, $V = U = 0$ and $W = 1$

As $Z = 0$, S $< R < 1$, $U = 1$, at $Z = 0, P = 0$ (13)

3. Solution of the Problem

It is possible to see the numerical analysis and methodology adopted here as parallel continuation of the work Coney and El-Shaarawi [12]. These different representations are created using the mesh network in figure 2. The grid size is denoted by ΔR and ΔZ which stands for radial and axial direction respectively.

$$V_{i+1,j+1} = V_{i,j+1}\left(\frac{S+i\Delta R}{S+(i+1)\Delta R}\right) - \frac{\Delta R}{4\Delta Z}\left(\frac{2S+(2i+1)\Delta R}{S+(i+1)\Delta R}\right)\left(U_{i,j+1} + U_{i+1,j+1} - U_{i,j} - U_{i+1,j}\right) \tag{14}$$

$$\frac{W_{i,j+1}^2}{S+i\Delta R} = \frac{(1-S)Re^2}{2T_a(1+S)}\frac{P_{i,j+1}-P_{i-1,j+1}}{\Delta R} \tag{15}$$

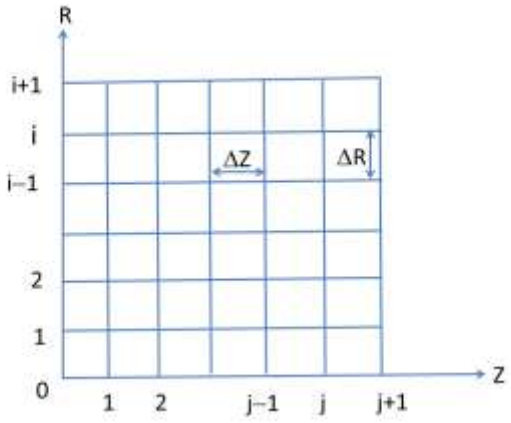

Figure 2. Grid construction for finite difference representations

$$V_{i,j}\left[\frac{W_{i+1,j+1}+W_{i+1,j}-W_{i-1,j}-W_{i-1,j+1}}{4\Delta R}\right]+U_{i,j}\left[\frac{W_{i,J+1}-W_{i,j}}{\Delta Z}\right]+\frac{V_{i,j}W_{i,j}}{N+i\Delta R}=$$

$$=\frac{W_{i+1,j+1}+W_{i+1,j}-2W_{i,j+1}-2W_{i,j}+W_{i-1,j}+W_{i-1,j+1}}{2(\Delta R)^2}+$$

$$\frac{W_{i+1,j+1}+W_{i+1,j}-W_{i-1,j}-W_{i-1,j+1}}{(S+i\Delta R)4\Delta R}-\frac{W_{i,j}}{(S+i\Delta R)^2}+\frac{2B}{S+i\Delta R} \quad (16)$$

$$V_{i,j}\left[\frac{U_{i+1,j+1}-U_{i-1,j+1}}{2\Delta R}\right]+U_{i,j}\left[\frac{U_{i,j+1}-U_{i,j}}{\Delta Z}\right]=$$

$$-\frac{P_{i+1,j}-P_{i,j}}{\Delta Z}+\frac{U_{i+1,j+1}-U_{i-1,j+1}}{(S+i\Delta R)2\Delta R}+\frac{U_{i+1,j+1}-2U_{i,j+1}+U_{i-1,j+1}}{(\Delta R)^2}+\frac{B}{S+i\Delta} \quad (17)$$

At R=1 and R=S, however, i=0 and i=m

Equation (12) results when the trapezoidal rule is applied.

$$\int_S^1 ru\,dr=\frac{\Delta R}{2}[Su_0,j+1u_m,j]+\Delta R\sum_{i=1}^{n-1}u_{ij}R_i \quad (18)$$

Boundary conditions (13) results $u_0,j=u_m,j=0$ and the above equation became to $\int_S^1 ru\,dr=\Delta R\ \sum_{i=1}^{m-1}u_{i,j}(S+i\,\Delta R)=\frac{1-S^2}{2}$

Through an iterative process, the collection of difference equations (14) to (18) has been resolved. Beginning with column j=0 and apply the equation (16) as a $1\leq i\leq m-1$, a set of algebraic linear equations is obtained. The numbers in the second column with j=1 for the velocity component W have been determined by solving this problem using the Gauss-Jordan method. Equations (15) and (17) are applied for $1\leq i\leq m-1$ and (18), Set of linear equations is obtained. We gather the velocity component's values U and pressure P in the column two with j is 1 by once more solving this problem using the Gauss-Jordan method. Lastly, the component's velocity values V in the next column $j=1$ have determined from the equation (14) by a Gauss-Jordan's technique the current values of U. By continuing the

process, we travel round the annulus axial direction, column by column, till the flow is complete formed both axially and tangentially.

4. Results and Discussion

The Bingham number B, aspect ratio S, and other parameters have all undergone numerical calculations for all acceptable values, as indicated in Table 1. Figures 3-26 depicts the velocity and pressure distribution around with direction of radial flow as outer wall for the annuli rotation.

Table 1. A list of the different parameters that were used

Aspect ratio S	Axial location Z	Rt	Bingham numeral B
0.4	0.03,0.04	20	0, 5, 10, 15
0.6	0.03,0.04	20	0, 5, 10, 15
0.9	0.03,0.04	20	0, 5, 10, 15

The growth of the component of the tangential velocity profile W for S=0.4, 0.6, 0.9 at various axial location of Z=0.03, 0.04 also for various non-Newtonian Bingham numerals B values is shown in the below Figures 3 to 8. Here, Rt is the parameter, which represents the relationship between the Reynolds and Tayler numbers, is set to 20. Tangential velocity values grow in the annulus from the wall of the inner cylinder to the wall of the outer cylinder wall. Additionally, it is discovered that the tangential velocity profile grows as aspect ratio S rises. That is, when the annuli's spacing is short, the tangential velocity is higher. Furthermore, it's discovered that tangential velocity profile grows as the Bingham number increases. This indicates that when the outer cylinder is rotating, the tangential velocity for thick viscous fluids tends to increase. It can be shown from the calculated outcomes for different numbers of Rt that the parameter Rt has very little impact on the tangential velocity.

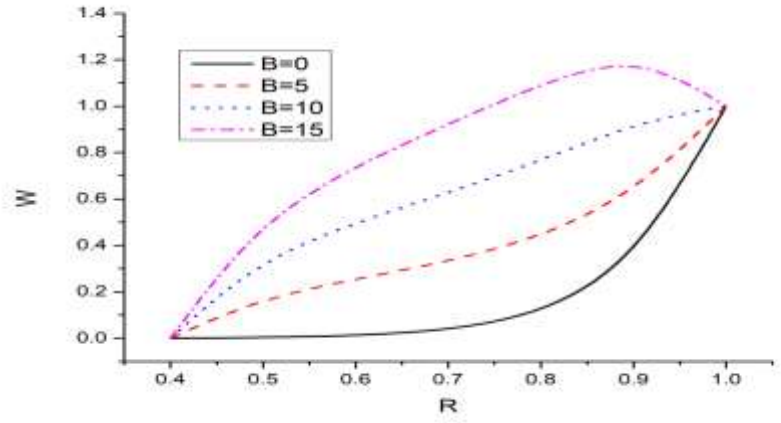

Figure 3: S=0.4 at Z=0.03 for tangential velocity profile.

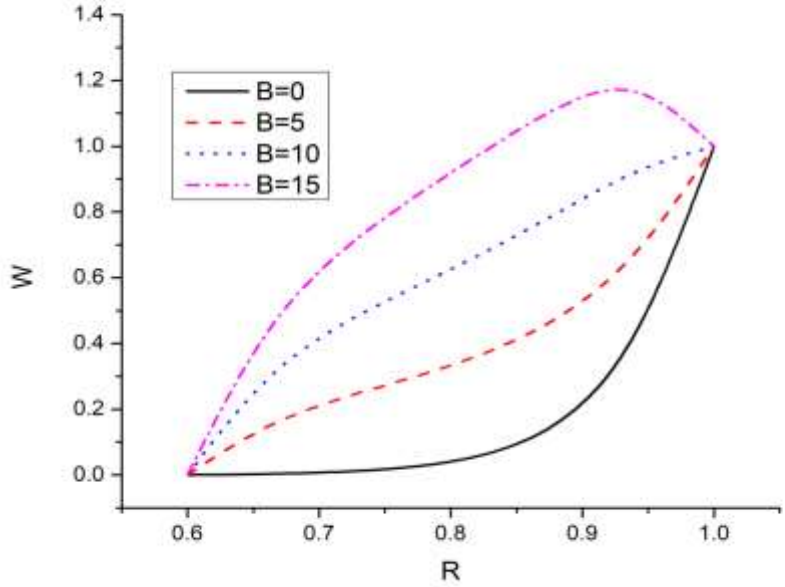

Figure 4: S =0.6 at Z =0.03 for tangential velocity profile.

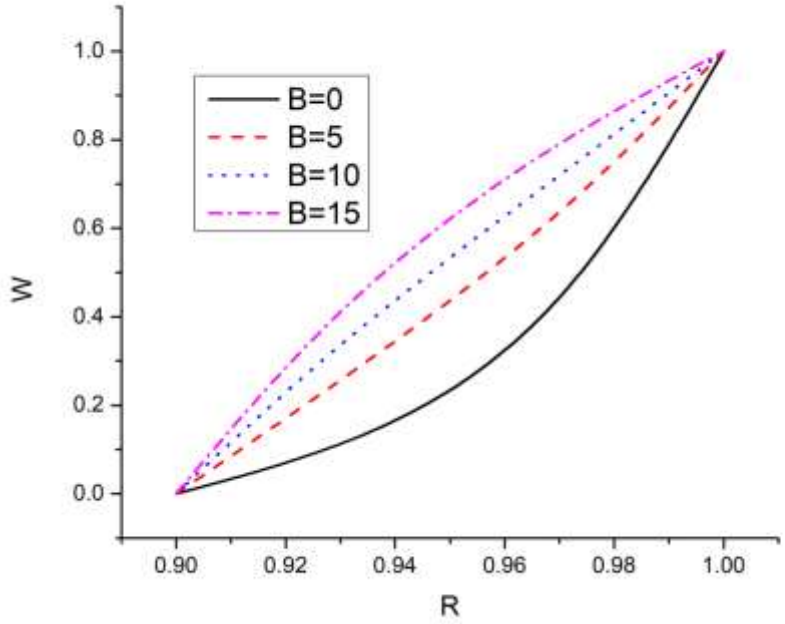

Figure 5: S =0.9 at Z =0.03 for tangential velocity profile.

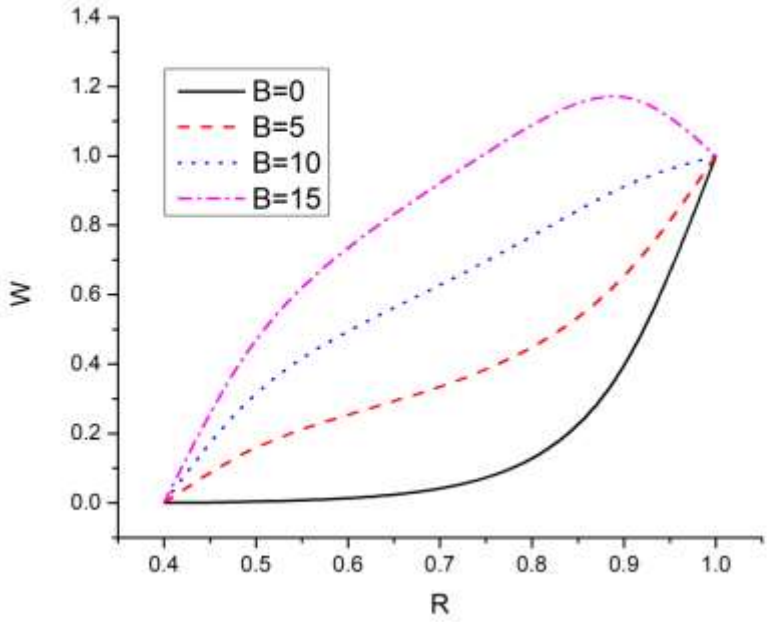

Figure 6: S =0.4 at Z =0.04 for tangential velocity profile.

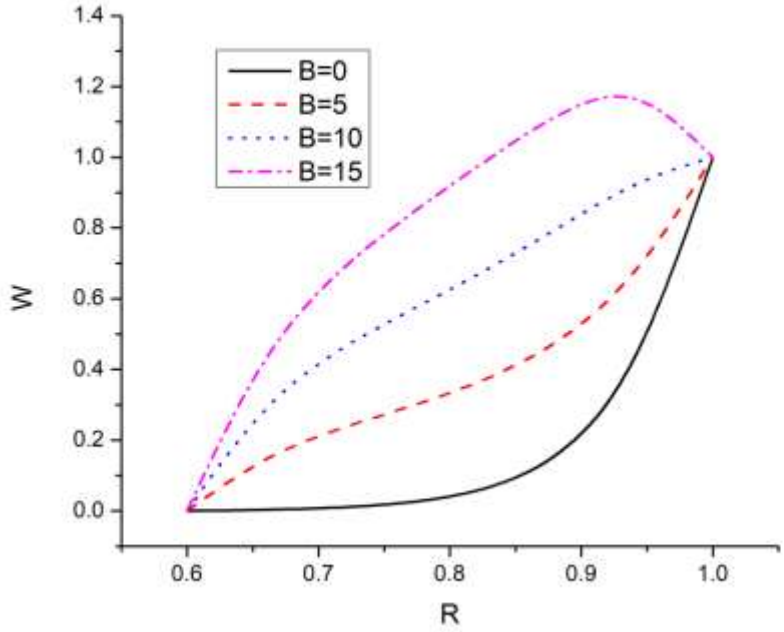

Figure 7: S=0.6 at Z =0.04 for tangential velocity profile.

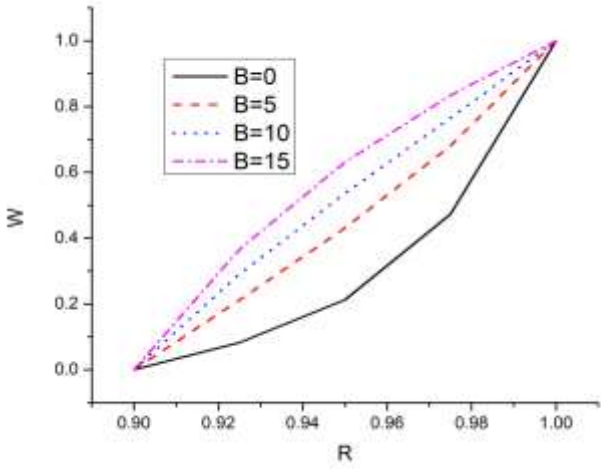

Figure 8: S =0.9 at Z =0.04 for tangential velocity profile.

Fig 9 to fig 14 illustrates the evolution of the axial velocity profile's component's U for S=0.4, 0.6, and 0.9 at axial coordinates of Z=0.03, 0.04, and for various Bingham numbers B values. To investigate the impact of the outer cylinder's rotation, calculations were performed over a range of Rt values. These figures display the values corresponding to Rt=20. It is shown that the component velocity U grows together with the Bingham value B and an aspect ratio S. When the Bingham number B hits zero, It's also demonstrated that a parabolic shape is taken by the velocity profile for both the stationary outer cylinder (Rt=0) and the spinning outer cylinder (Rt=20). The observed results, however, show that the rotation's impact on the axial velocity component is relatively minimal. In this case, our results for B=0 agree with those of Coney and El-Shaarawi[12] and Rt=0 with several Bingham numerals conform to the outcomes of Kandasamy [7].

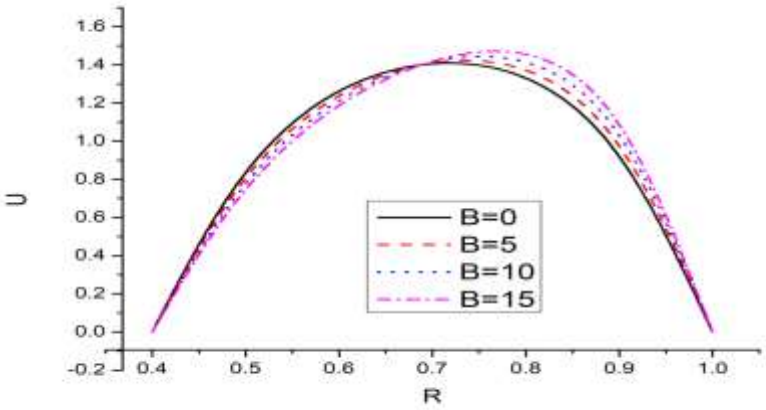

Figure 9: S =0.4 at Z =0.03 for axial velocity profile.

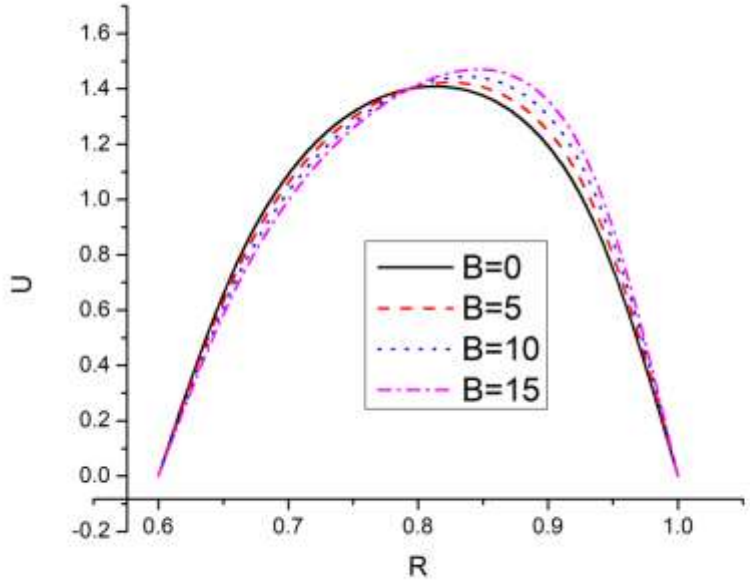

Figure 10: S =0.6 at Z =0.03 for axial velocity profile.

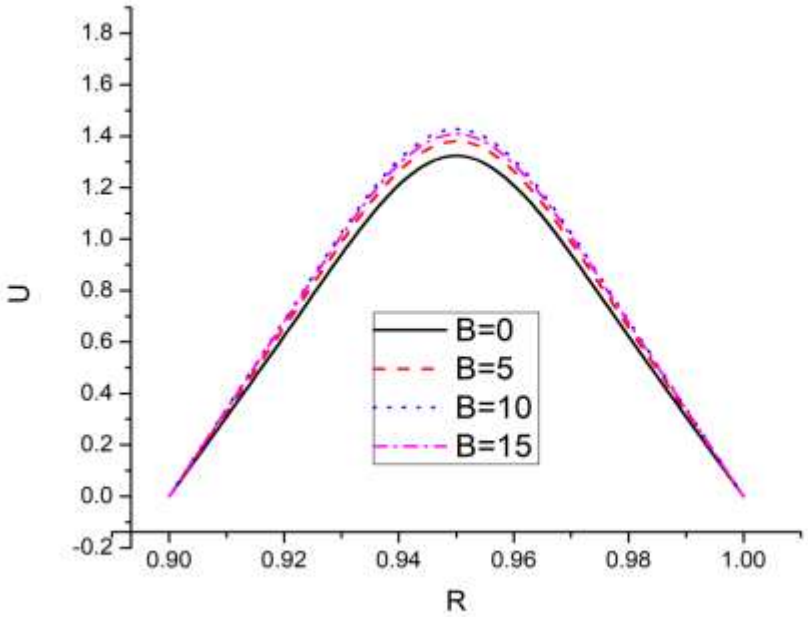

Figure 11: S =0.9 at Z =0.03 for axial velocity profile.

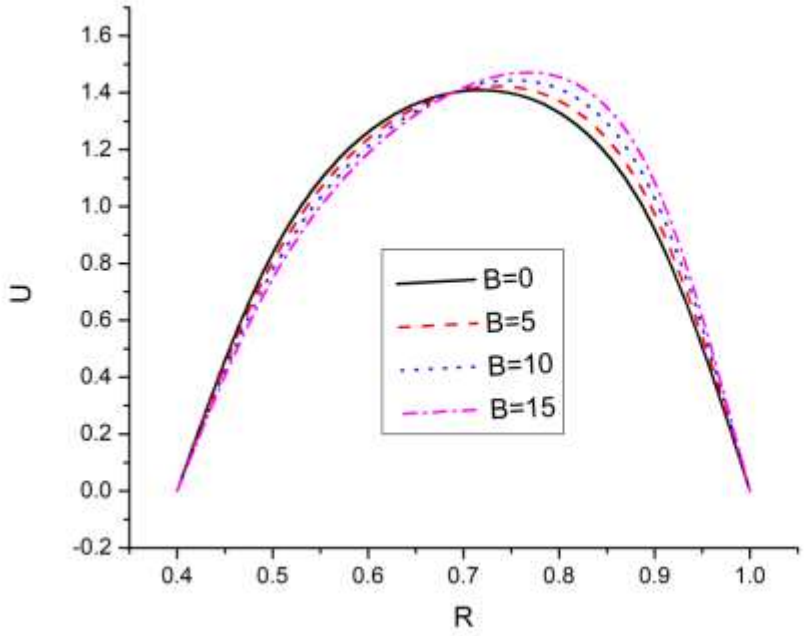

Figure 12: S =0.4 at Z =0.04 for axial velocity profile.

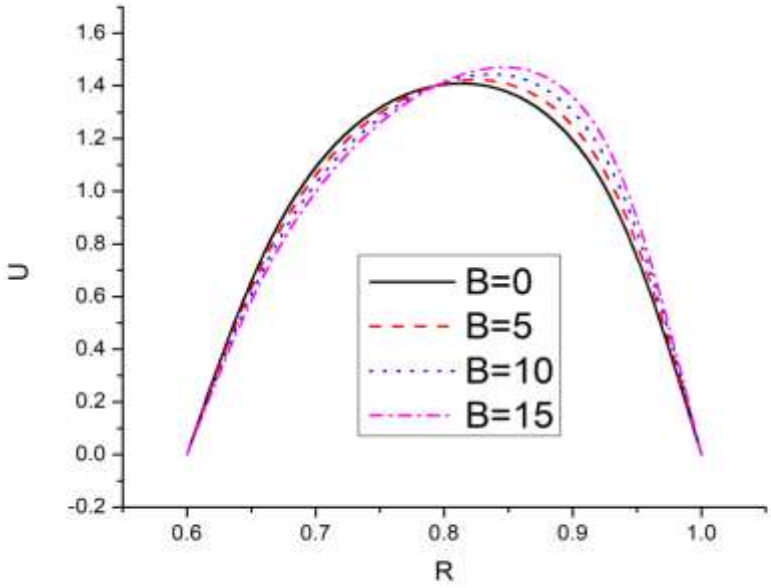

Figure 13: S =0.6 at Z =0.04 for axial velocity profile.

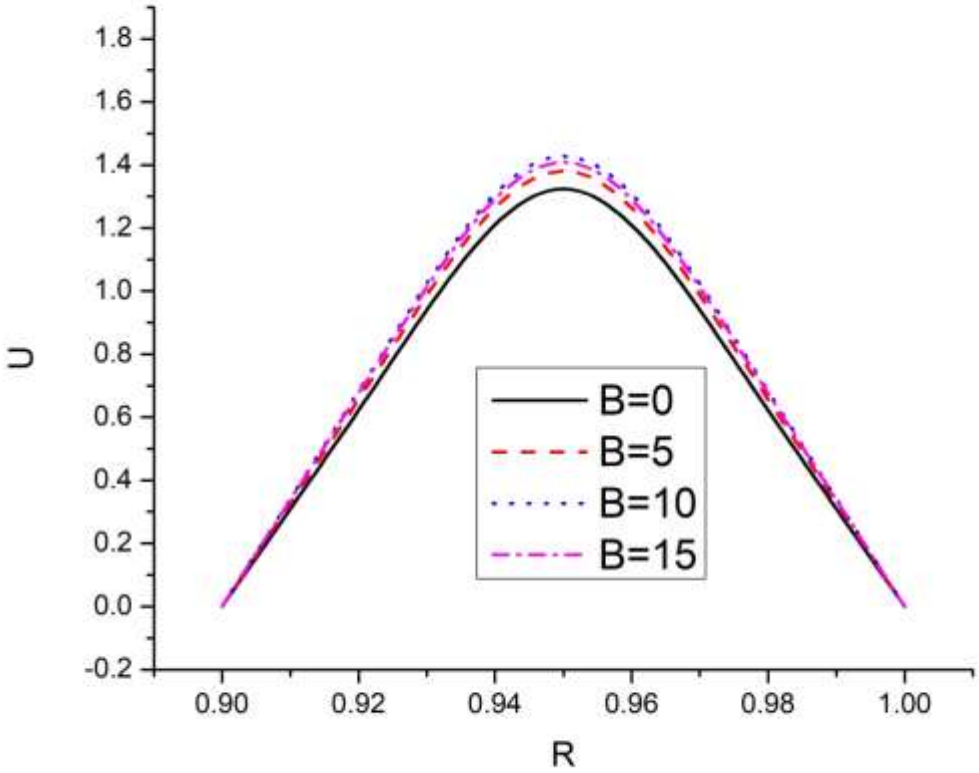

Figure 14: S =0.9 at Z =0.04 for axial velocity profile.

Figure 15 to 20 shows Radial velocity profile V for S=0.4, 0.6, 0.9 for various values of non-Newtonian Bingham numerals B at the axial positions of Z =0.03, 0.04. For computational purposes, the parameter values Rt are assumed to be 0 in additional to 20. Radial velocity values are negative near the inner cylinder wall because it is moving in the opposite direction as the radial coordinate R, while they are positive near the outer cylinder wall because it is moving in the same direction as the radial coordinate. At any cross section of the axis, the values of the radial velocity decreases as Rt and Bingham number B increases. The outcomes of specific circumstances like Rt=0, B=0 are completely consistent with past studies [7, 12] respectively.

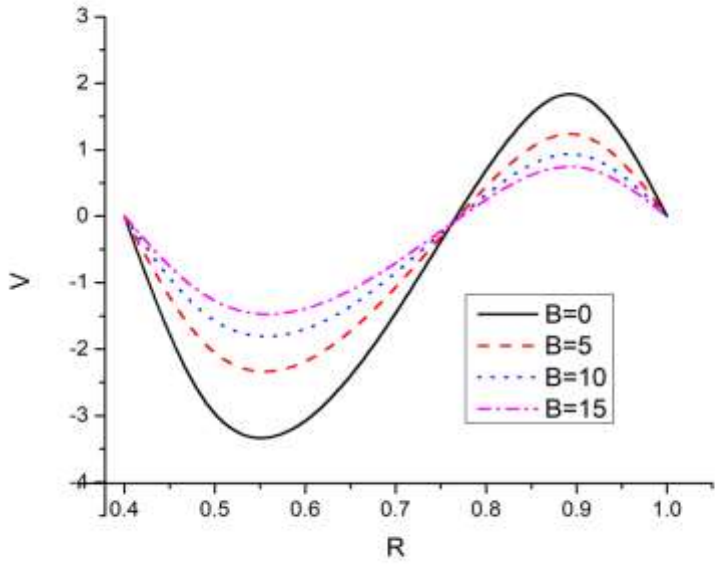

Figure 15: S =0.4 at Z =0.03 for radial velocity profile.

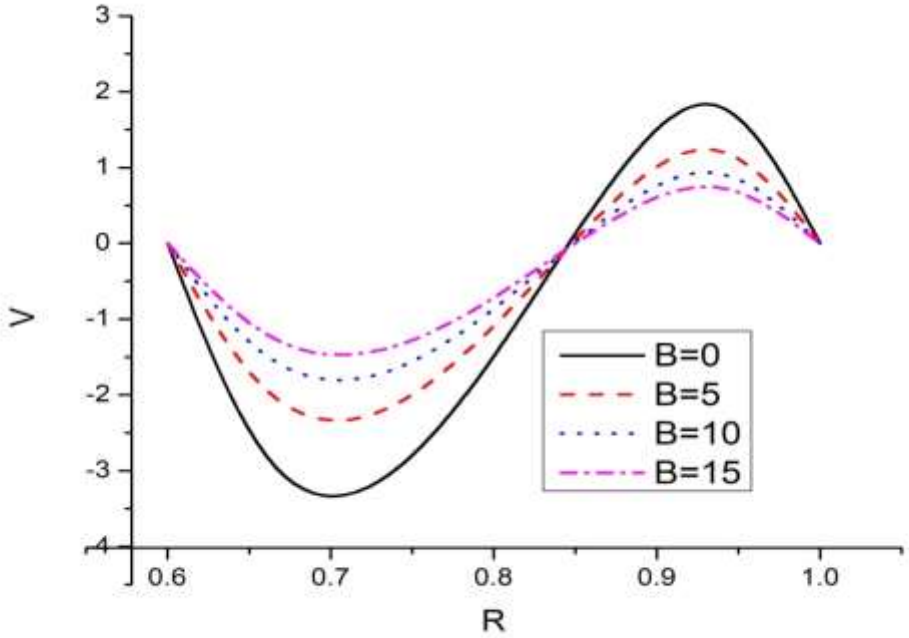

Figure 16: S =0.6 at Z =0.03 for radial velocity profile.

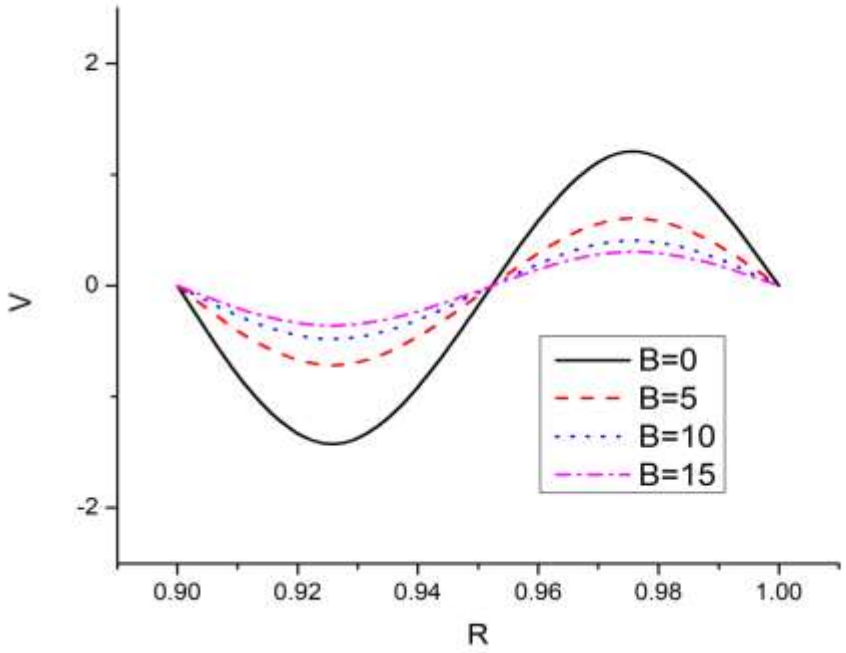

Figure 17: S =0.9 at Z =0.03 for radial velocity profile.

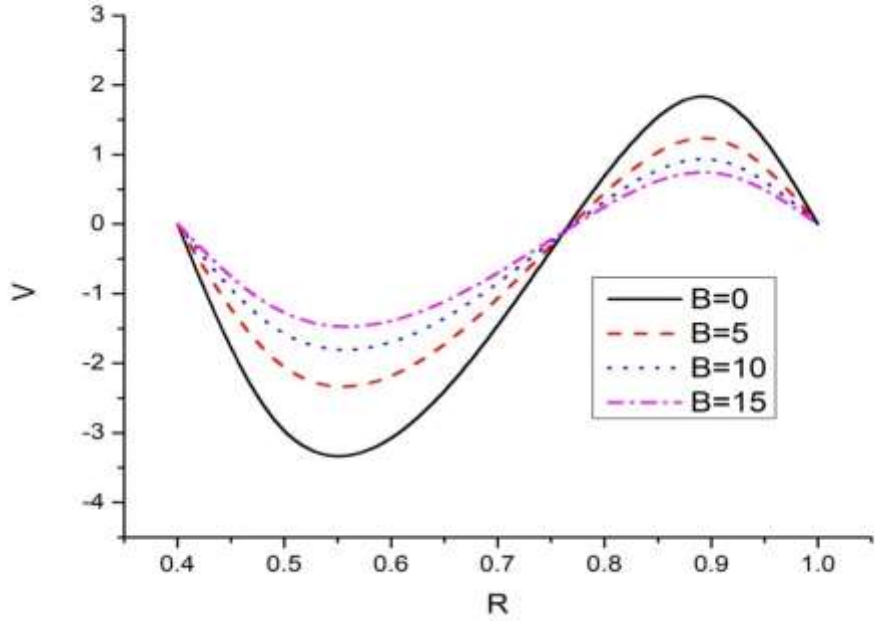

Figure 18: S =0.4 at Z =0.04 for radial velocity profile.

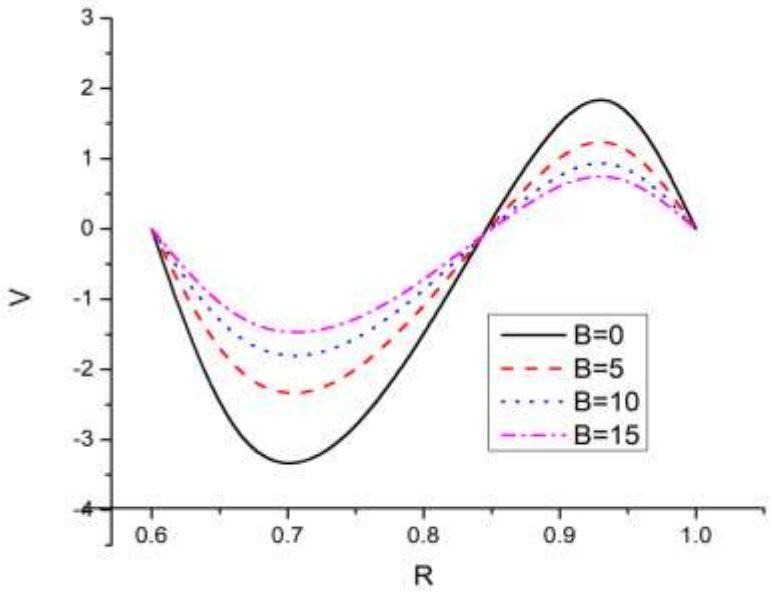

Figure 19: S =0.6 at Z =0.04 for radial velocity profile.

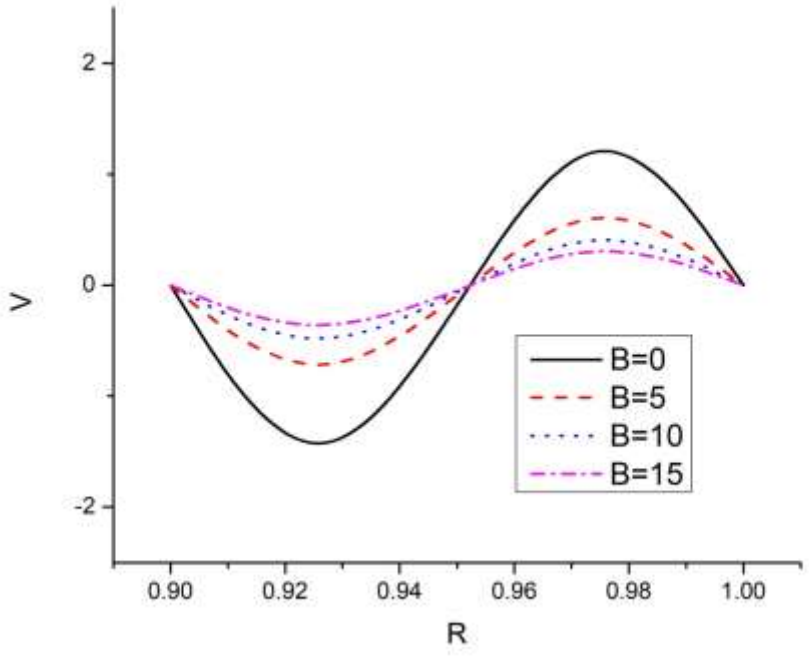

Figure 20: S =0.9 at Z =0.04 for radial velocity profile.

Figure 21 to 23 displaying the distribution of the pressure P along with the radial coordinate R for same values of parameters. It is found that the values of P increases from a maximum at the inner wall to a minimum at the outer wall. Additionally, it's also discovered that as Bingham values increases, the values of pressure P increases as well. This is due to thick, viscous fluids typically have higher pressures. Additionally, it is noted that the pressure slowly becomes irrespective of the radial coordinate in the region close to the inner wall. At any cross section, the impact of outer cylinder rotation on fluid pressure appears to be minimal or low. The results in this case for B=0 and Rt=0 accord with the preceding findings [7, 12] correspondingly.

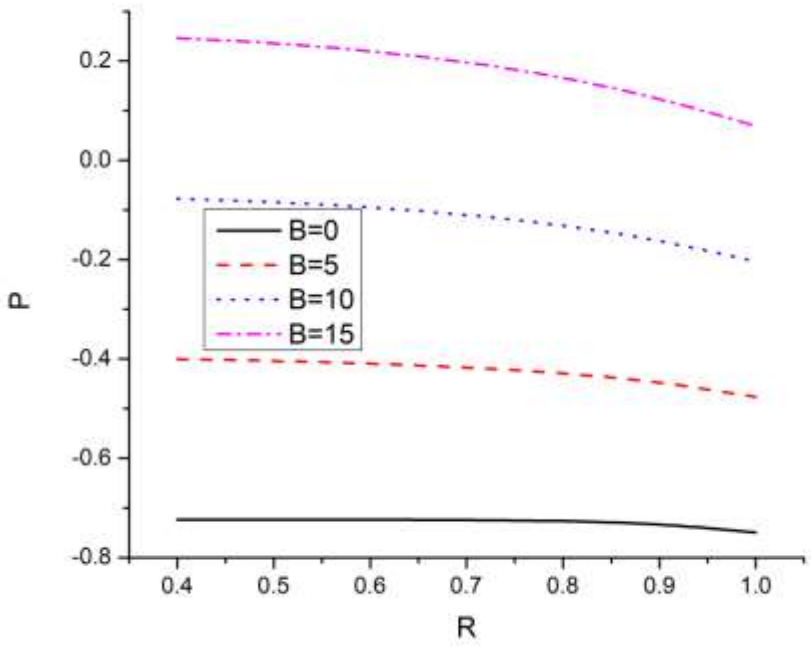

Figure 21: S =0.4 at Z =0.03 for pressure distribution.

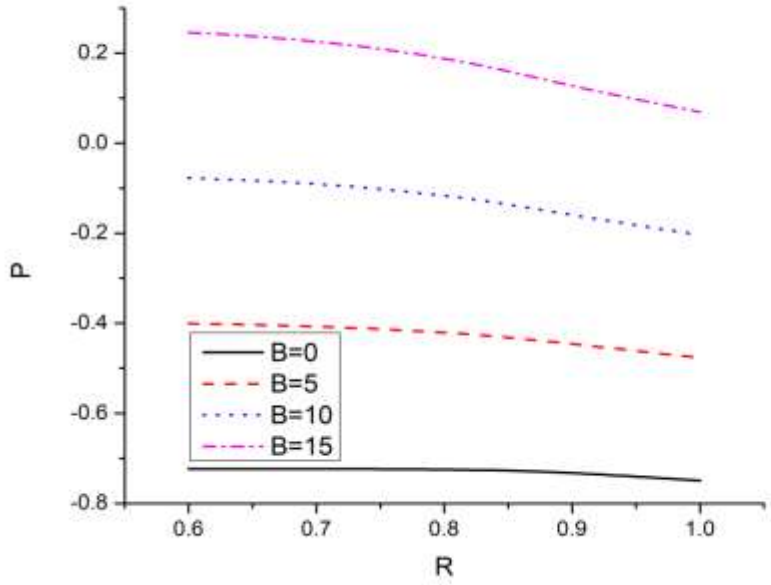

Figure 22: S =0.6 at Z =0.03 for pressure distribution.

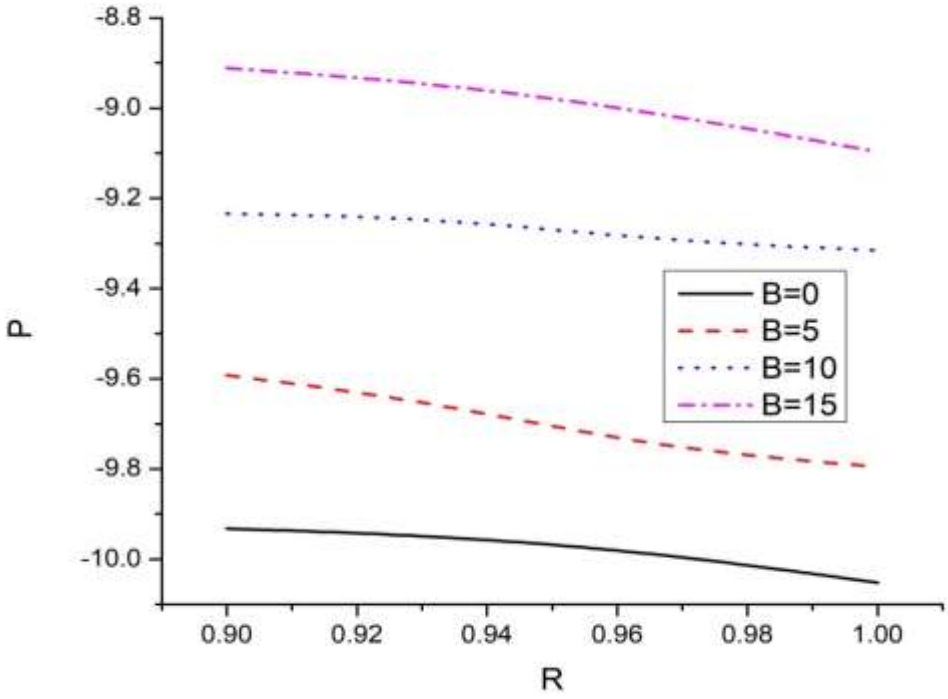

Figure 23: S =0.9 at Z =0.03 for pressure distribution.

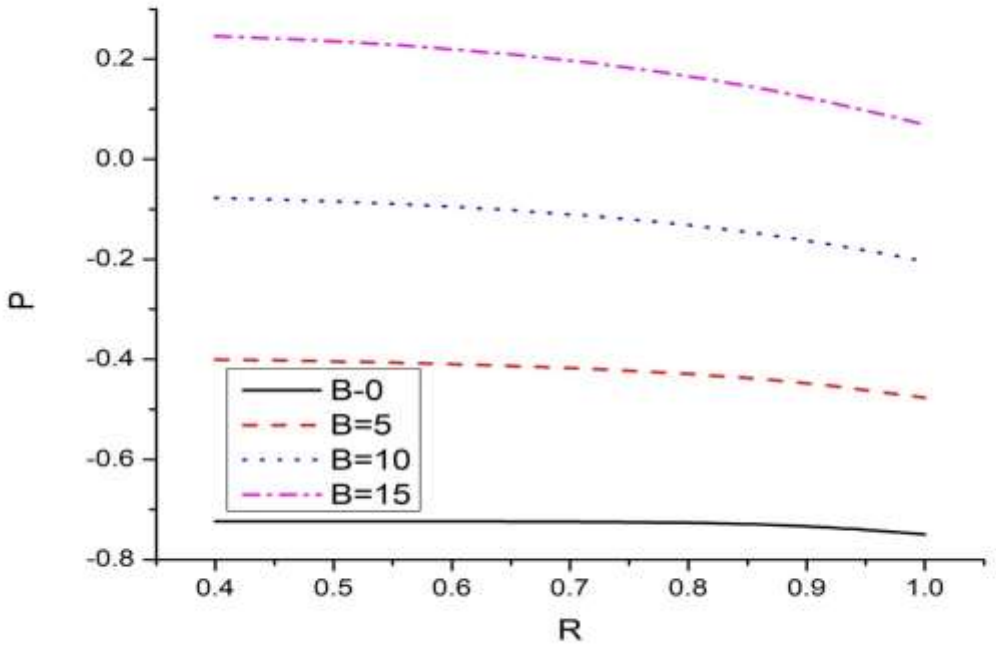

Figure 24: S =0.4 at Z =0.04 for pressure distribution.

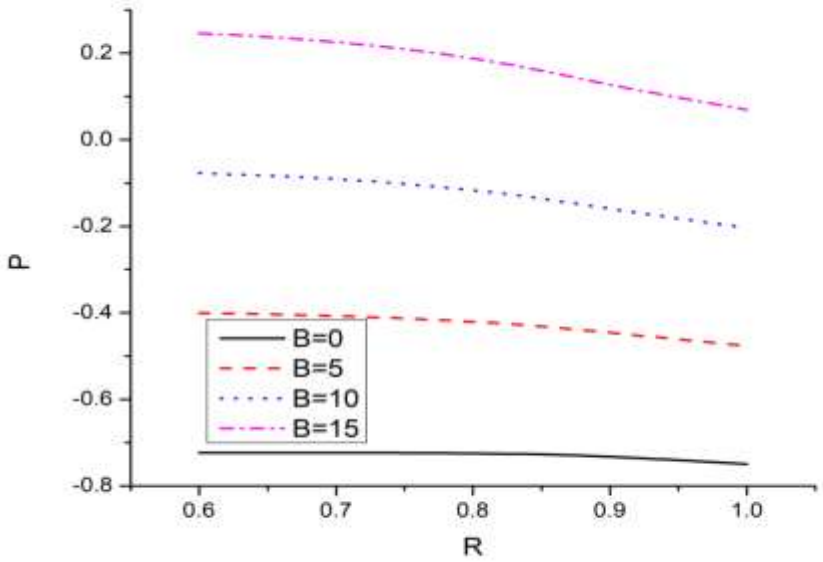

Figure 25: S =0.6 at Z =0.04 for pressure distribution.

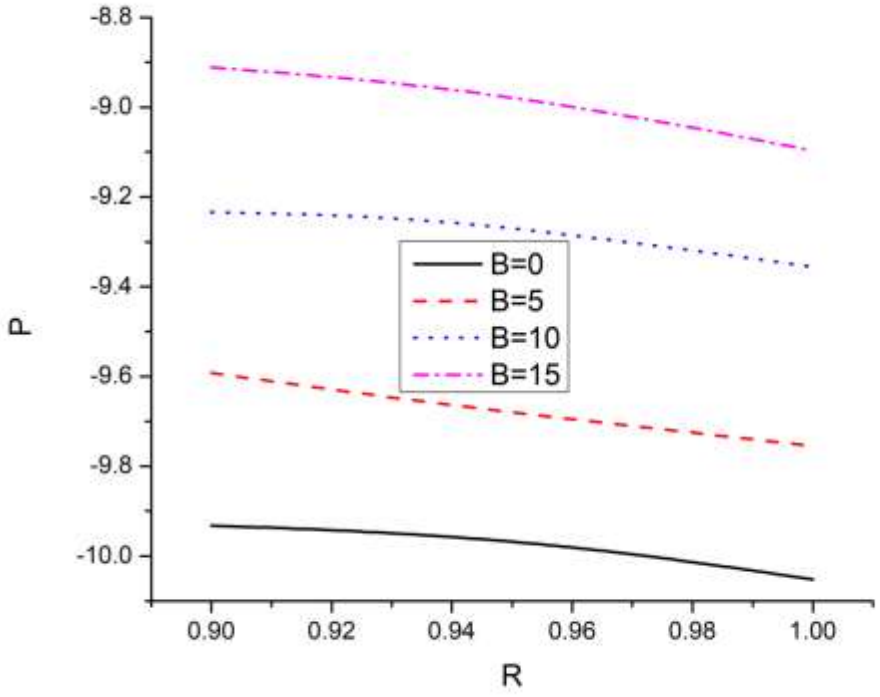

Figure 26: S =0.9 at Z=0.04 for pressure distribution.

5. Conclusions

Concentric annuli flow in the area at the entrance with a rotating outer cylinder for the Bingham non-Newtonian fluid was presented using numerical results. Study is done on how the factors S, B, and Rt affect the velocity profiles and the pressure distribution. All Bingham number B acceptable values were calculated numerically, the aspect ratio S and parameter Rt. Geometric representations of the pressure and velocity distributions along the radial direction R were used. The current findings are discovered to be consistent with the findings matching to numerous specific situations described in the literature.

The study's findings lead to the following conclusion.

1. The annulus's tangential velocity increases from inner to outer walls.
2. The axial velocity component U grows with increasing aspect ratio S at all Bingham number B values.
3. It is discovered that radial velocity only depends on axial coordinate.
4. The pressure decreases from the annulus' outside wall, where it is at its highest, to the inner wall, when it is at its lowest.
5. It appears that the outer wall rotation has little significance on any of these flow parameters.

Refferences

1. Mishra, I. M., Surendra Kumar and Mishra, P.: Entrance region flow of Bingham plastic fluids in concentric annulus. Indian Journal of Technology, 23, (1985), 81- 87.
2. Batra, R. L. and Bigyani, D.: Flow of a Casson fluid between two rotating cylinders. Fluid Dynamic Research, 9, (1992), 133-141.
3. Maia, M. C. A. and Gasparetto, C. A.: A numerical solution for entrance region of Non-Newtonian flow in annuli. Brazilian Journal of Chemical Eng., 20, (2003), 201-211.
4. Sayed-Ahmed, M. E. and Hazem Sharaf-El-Din.: Entrance region flow of a power law fluid in concentric annuli with rotating inner wall. International Communications in Heat and Mass Transfer, 33, (2006), 654-665.
5. Kandasamy, A. and Srinivasa, R. N.: Entrance region flow in concentric annuli with rotating inner wall for Herschel-Bulkley fluids. International Journal of Applied and Computational Mathematics, 1, (2015), 235-249.
6. Kandasamy, A.: Entrance region flow heat transfer in concentric annuli for a Bingham fluid. In Proceedings of Third Asian-Pacific Conference on Computational Mechanics, Seoul, Korea, 1996, pp. 1697-170
7. Round, G. F. and Yu. S.: Entrance laminar flows of viscoplastic fluids in concentric annuli. The Canadian Journal of Chemical Engineering, 71, (1993), 642-645.
8. Batra, R. L. and Bigyani Jena: Entrance region flow of blood in concentric annulus. International Journal of Engineering Science, 28, (1990), 407-419
9. Rekha G. Pai and Kandasamy, A.: Entrance region flow of Bingham fluid in an annular cylinder. International Journal of Applied Engineering Research, 5, (2014), 7083- 7101.
10. Schlichting, H. and Gersten, K.: Boundary Layer Theory. 8th ed, Springer, 2000.
11. Coney, J. E. R. and El-Shaarawi, M. A. I.: A contribution to the numerical solution of developing laminar flow in the entrance region of concentric annuli with rotating inner walls. Journal of Fluids Engineering, 96, (1974), 333-340.
12. R.L. Batra and Bigyani Das.: Flow of a Casson fluid rotating cylinders International journal of Fluid Dynamics Research. 9 (1992) 133-141.
13. Bird, R. D., Dai, G. C. and Yarusso, B. J.: The rheology and flow of viscoplastic materials. Reviews in Chemical Engineering, 1, (1982), 1-70.